The Planetary Science Journal, 6:232 (15pp), 2025 October https://doi.org/10.3847/PSJ/ae0465

The Lunar Instrumentation for Subsurface Thermal Exploration with Rapidity (LISTER) on Blue Ghost Mission 1 to Mare Crisium. I. Pneumatic Excavation of Regolith

S. Nagihara[1], K. Zacny[2], P. Ngo[2], L. Sanasarian[2], R. Misra[2], M. Zasadzien[2], V. Sanigepalli[2], M. Schmitt[2], A. Wang[2], C. Ladd[2], A. Shmavonian[2], P. Ng[2], Y. Hwang[2], W. Garcia[2], J. Knorr[2], R. Tuanuma[2], T. Thomas[2], H. Jung[2], X. Estey[2], T. Colenbrander[2], X. Fries[2], J. Emery[2], N. Jeevanjee[2], C. Castle[2], N. Sadagopan[2], T. Heiman[2], E. Killian[2], N. Steele[2], Y. Matsuyama[2], G. Paulsen[2], M. Grott[3], J. Knollenberg[3], T. L. Hudson[4], S. E. Smrekar[4], and M. A. Siegler[5]
[1] Department of Geosciences, Texas Tech University, Lubbock, TX 79423, USA; seiichi.nagihara@ttu.edu
[2] Honeybee Robotics, Altadena, CA 91001, USA
[3] German Aerospace Center (DLR), Institute of Space Research, Berlin, Germany
[4] Jet Propulsion Laboratory, California Institute of Technology, Pasadena, CA 91109, USA
[5] Hawaii Institute of Geophysics and Planetology, University of Hawaii, HI 96822, USA
Received 2025 July 7; revised 2025 August 25; accepted 2025 September 3; published 2025 October 8

Abstract

The Lunar Instrumentation for Subsurface Thermal Exploration with Rapidity (LISTER) is the first robotically deployed subsurface thermal probe that actively excavates lunar regolith and makes scientific measurements at multiple depths. It was deployed in Mare Crisium on Blue Ghost Mission 1 in 2025 March, reached 1 m depth, and measured the temperature and thermal conductivity of the regolith at eight different depths. The previous depth record for robotic in situ thermal measurements of the Moon was 8 cm. LISTER utilizes the pneumatic excavation technique, blowing a jet of pressurized nitrogen gas, as it pushes its thermal probe into the regolith. The gas expands rapidly in the lunar vacuum and lofts regolith clumps and clasts out of the hole. When the probe reaches one of the depths targeted for thermal measurements, LISTER stops blowing gas and pushes the probe into the yet-to-be-excavated bottom-hole regolith. It completes the necessary thermal measurements in 2 hr and then resumes excavation to the next targeted depth. LISTER detects obstacles on its way by monitoring the weight on bit (WOB). When the WOB exceeds a programmable threshold, LISTER attempts to dislodge the obstacle by automatically performing a piston-like vibratory movement ("dithering"), while it keeps blowing gas. Finally, video-monitoring the ejecta from LISTER's excavation operations is useful in studying the stratigraphy of the regolith.

Unified Astronomy Thesaurus concepts: The Moon (1692); Lunar regolith (2315)

1. Introduction

On 2025 March 2, Firefly Aerospace became the first USA-based company to soft-land a robotic spacecraft in the upright position on the Moon. The Blue Ghost lander deployed 10 payloads in Mare Crisium (Figure 1) under NASA's Commercial Lunar Payload Services (CLPS) program. The Lunar Instrumentation for Subsurface Thermal Exploration with Rapidity (LISTER) was one of the payloads (Figures 2 and 3). On this mission, LISTER became the first robotically deployed probe that pneumatically excavated regolith to carry out multiple scientific measurements in the subsurface of an extraterrestrial body. LISTER reached 1 m depth into the regolith of Mare Crisium and measured temperature and thermal conductivity of the regolith at eight different depths (0.288, 0.329, 0.394, 0.6, 0.783, 0.947, 0.956, and 0.971 m depths). This article describes the LISTER instrumentation and the first pneumatic subsurface excavation ever performed on the Moon. The analysis of subsurface thermal data acquired during the mission is presented in another article.

LISTER has been developed to quantify the flow of heat that originates from the interior (aka the endogenic heat flow) of the Moon at its landing site. The endogenic heat flow is one of the key pieces of information necessary in unraveling the thermal evolution history of the rocky planets and moons (e.g., National Academies of Sciences, Engineering, and Medicine 2023). It can be measured accurately only in situ by landing a spacecraft and deploying a probe to the subsurface. The probe measures the temperature and thermal conductivity of the regolith/rock at multiple depths. Heat flow is then obtained as a product of the thermal gradient and the thermal conductivity of the depth interval penetrated by the probe. The measurements must be made deep enough in the subsurface, where the temperature of the regolith (or rock) is not significantly affected by the annual and diurnal insolation cycles. The minimum depth required for such measurement varies, depending on the periods of the insolation cycles and the thermal conductivity of the regolith (or rock). For the Moon, it is 1–1.5 m depth, based on data from the Apollo heat flow experiments (M. G. Langseth et al. 1976). For Mars, it has been estimated to be 3–5 m depth (M. Grott et al. 2007; M. A. Siegler et al. 2017; T. Spohn et al. 2018).

It has been suggested that heat flow may be estimated from passive microwave observations from either Earth or lunar orbit (F. P. Schloerb et al. 1976; M. A. Siegler et al. 2023). The thermal gradient below 1 m depth can be estimated from microwaves below ~3 GHz, but thermal conductivity cannot. Additionally, the microwave emission from the lunar surface is

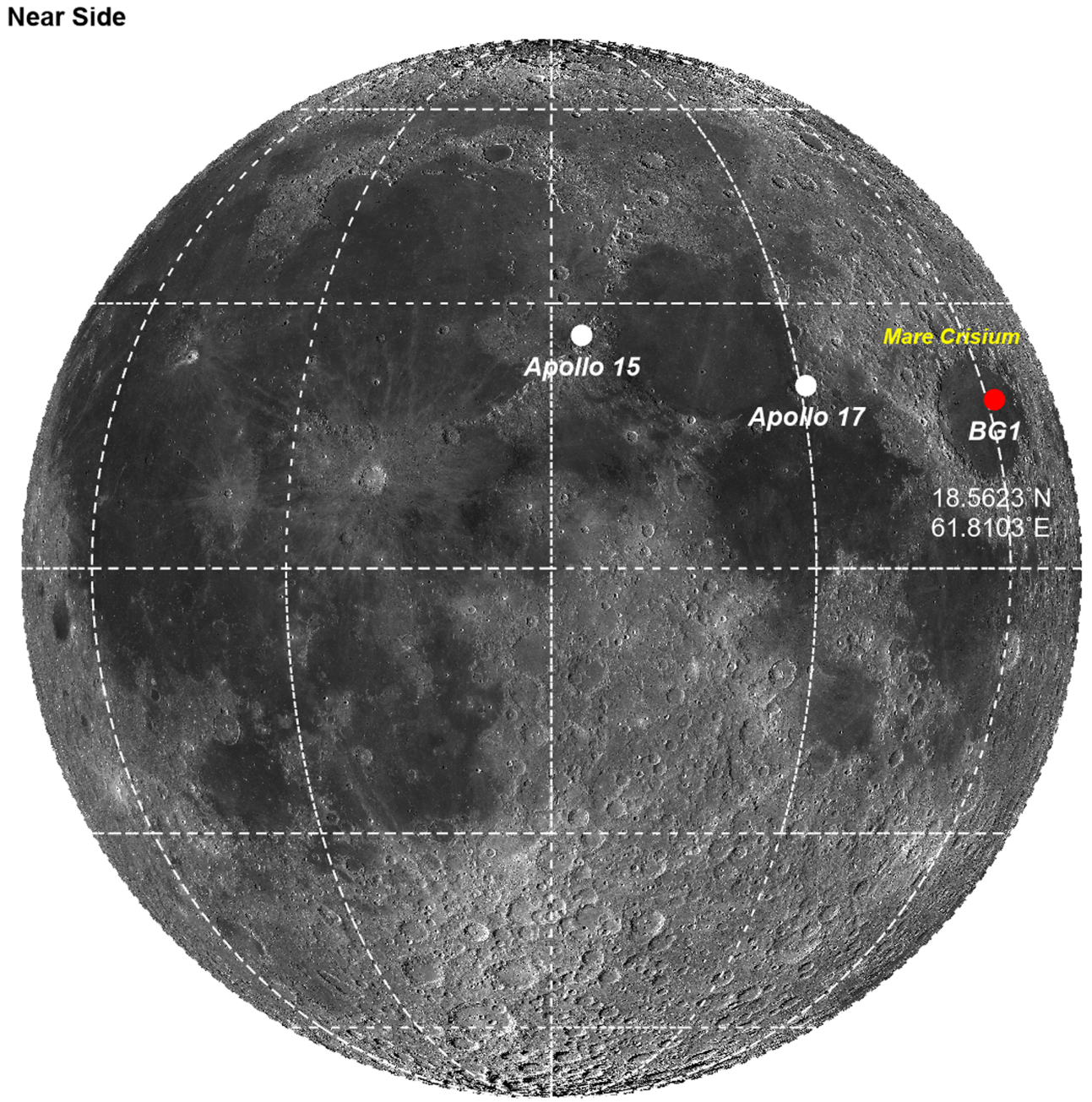

Figure 1. The landing site of Blue Ghost Mission 1 (BG1) along with the Apollo 15 and 17 lander locations on the global nearside mosaic of the Lunar Reconnaissance Orbiter Wide Angle Camera images. Astronauts used handheld rotary-percussive drills to deploy heat flow probes at Apollo 15 and 17.

affected by many other local factors such as topography and the physical properties of the regolith (S. J. Keihm 1984). This method is still experimental and needs ground-truthing by physical in situ measurements of heat flow.

So far, the Moon is the only extraterrestrial body where endogenic heat flow has been determined successfully. The Apollo astronauts, using a rotary-percussive drill, excavated a hole, one half-meter section at a time, and then inserted the heat flow probe (M. G. Langseth et al. 1976). The Apollo 15 (Figure 1) astronauts drilled two such holes to 1.5 m and 1.1 m depths. Apollo 17 went deeper, reaching 2.4 m depth with an improved auger design. To unravel the thermal evolution history of the Moon, endogenic heat flow needs to be determined at many additional locations. It would be far more economical if this could be done on robotic missions rather than relying on human missions. However, no such attempt has been made on robotic lunar-landing missions since the Apollo era, because it has been a major technological challenge to robotically deploy a probe deep enough into the subsurface to quantify endogenic heat flow. The conventional drilling technique used by the Apollo astronauts is too complex to be implemented on a small robotic lander like Blue Ghost (2 m tall, 3.5 m wide, 469 kg dry mass; Firefly Aerospace 2025).

It should be noted, however, that there have been robotic lunar-landing missions that collected core samples using conventional drills. Luna 16, 20, and 24 recovered cores from 0.35 m, 0.27 m, and 2 m depths, respectively (A. P. Vinogradov 1971; G. Heiken & M. C. McEwen 1972; V. L. Barsukov 1977). Chang'e-5 and −6 also collected drill cores from 1 m and 1.5 m depths,

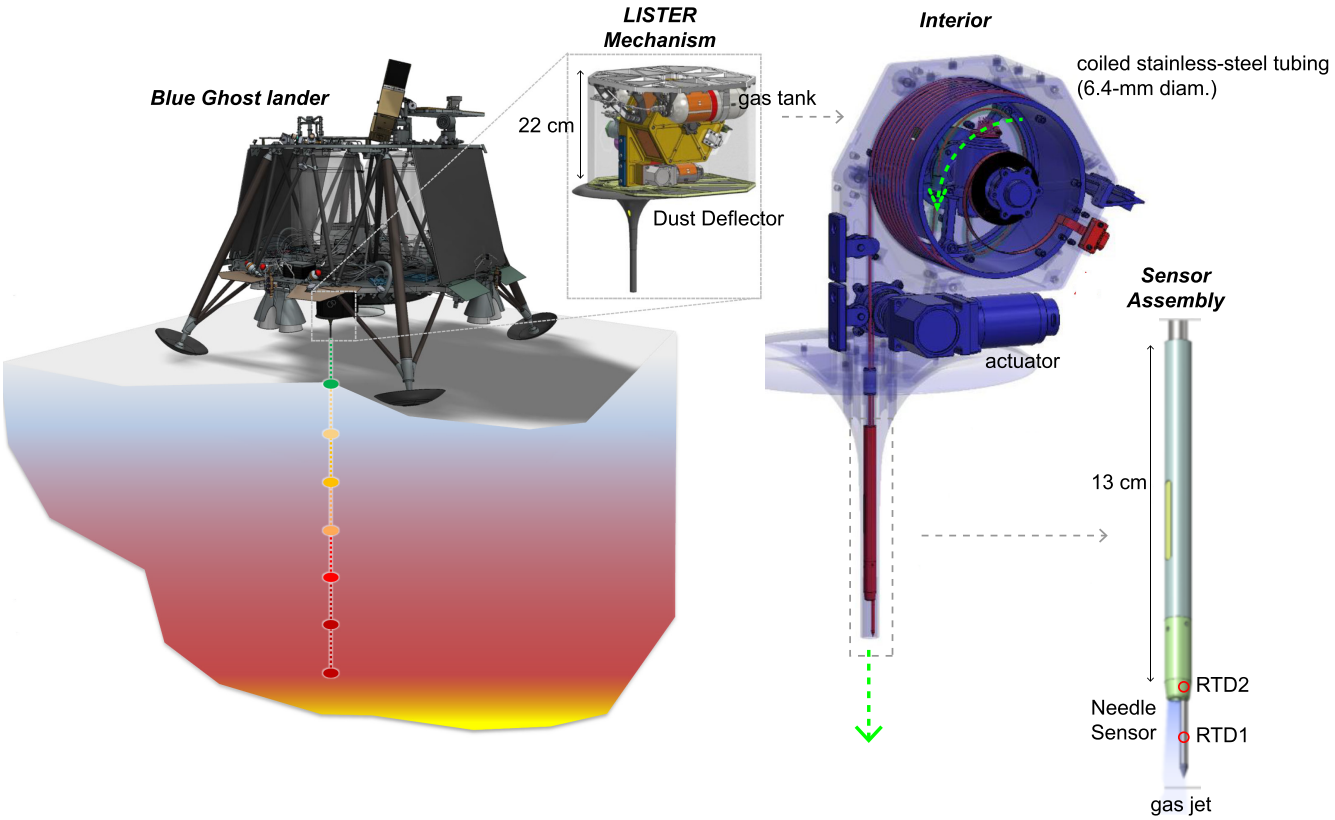

Figure 2. A conceptual drawing of the LISTER deployment mechanism accommodated below the platform of the Blue Ghost lander as it makes thermal measurements at multiple depths into the subsurface (left). Schematic drawings of the interior of LISTER's deployment mechanism (middle) and sensor assembly (right) are also shown. A photograph of the mechanism is shown in Figure 3.

respectively (T. Zhang et al. 2023; Y. Zheng et al. 2023). These missions did not conduct in situ scientific measurements in the subsurface. The landers were about 3 times as large and massive as Blue Ghost (A. A. Siddiqi 2018).

Prior to LISTER, three subsurface thermal probes flew on robotic space missions. Two of them (MUPUS on Rosetta and ChaSTE on Chandrayaan-3) were lance-tip probes and were not designed to reach sufficient depths to measure the endogenic heat flow of the target bodies (T. Spohn et al. 2007; N. Mathew et al. 2025). ChaSTE was deployed on the Moon and reached 8 cm depth. The heat flow and physical properties probe on the InSight mission to Mars was intended to reach 5 m depth to quantify the endogenic heat flow (T. Spohn et al. 2018). It relied on the so-called "mole" to penetrate Mars regolith. The mole was a cylindrical device with 2.7 cm diameter and 40 cm length. It was designed to use the momentum generated by internal hammering in wedging itself into the regolith. However, the physical properties of the regolith at the InSight landing site were not compatible with this penetration method. The mole was not able to fully submerge itself into the regolith (T. Spohn et al. 2022a; 2022b).

These predecessors of LISTER attempted to push themselves into the subsurface by compacting the soil around them. On the Moon, such methodology falls short, because the regolith is already well compacted and cohesive. Its relative density can be over 80% at depths as shallow as 0.2 m (W. D. Carrier et al. 1991). In other words, very little room for penetration can be created by simply compacting regolith. To penetrate deep, a probe must actively excavate a hole, but how can it be done without exceeding the limited payload mass and power capacity of small robotic landers?

LISTER is the first robotically deployed subsurface probe that actively excavates regolith. It blows a jet of pressurized nitrogen gas (>99.999% purity) at the regolith. The gas expands rapidly in the lunar vacuum and lofts regolith clumps and clasts out of the hole (E. Mumm et al. 2010; K. Zacny et al. 2013). This pneumatic technique should not be confused with the commercial pneumatic drills (aka air drills) often used in construction work. These power tools use pressurized air (supplied from an external air compressor) in place of an electric motor in actuating a rotary-percussive or percussive drill bit. LISTER's pneumatic excavation technique uses gas alone without any mechanical cutting or grinding, as we explain in detail in the following sections.

On the Blue Ghost mission, we were aided by several cameras set up below the lander's platform to monitor the LISTER operations. Two of those were color video cameras operated by Firefly, and four of them were a part of the Stereo CAmeras for Lunar Plume Surface Studies (SCALPSS) payload (M. E. Banks et al. 2022; O. K. Tyrrell et al. 2022) that captured black-and-white still images. Because LISTER operated while it was in the shadow of the lander's deck, a floodlight was used while the cameras operated. Unfortunately, the use of the video cameras was limited to the early stage of LISTER operations, because, as the spacecraft heated up toward mid-lunar-day, the cameras became inoperable. A limited number of still images were captured in the middle and late stages of LISTER operations.

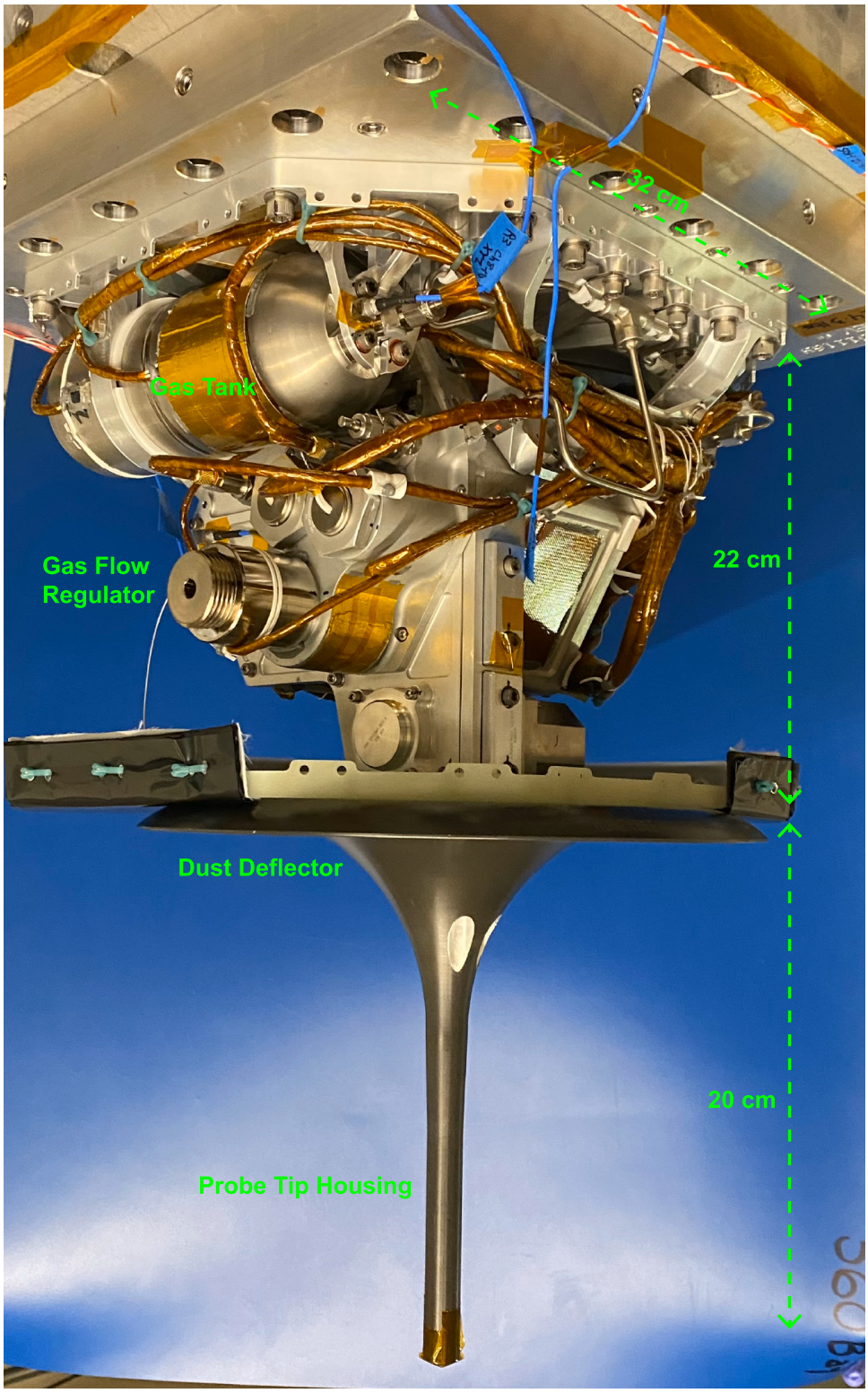

Figure 3. A photograph of the LISTER deployment mechanism with the needle sensor fully stowed.

2. Concept of Operations

The LISTER hardware consists of two units: the avionics that typically sit on the lander's deck and the deployment mechanism that is accommodated under the deck for proximity to the ground (Figures 2 and 3). The mechanism spools out a stainless-steel (S.S.) tube (6.4 mm diameter) pointing downward. As the tube spools out, the mechanism straightens it and pushes it downward. Compressed nitrogen gas is fed through the tube, as it penetrates the regolith below the lander. The gas jet, once released, rapidly expands in the lunar vacuum. Its momentum is used to loft regolith clumps and clasts out of the hole. The dust deflector protects the deployment mechanism and other equipment from the objects ejected from the hole.

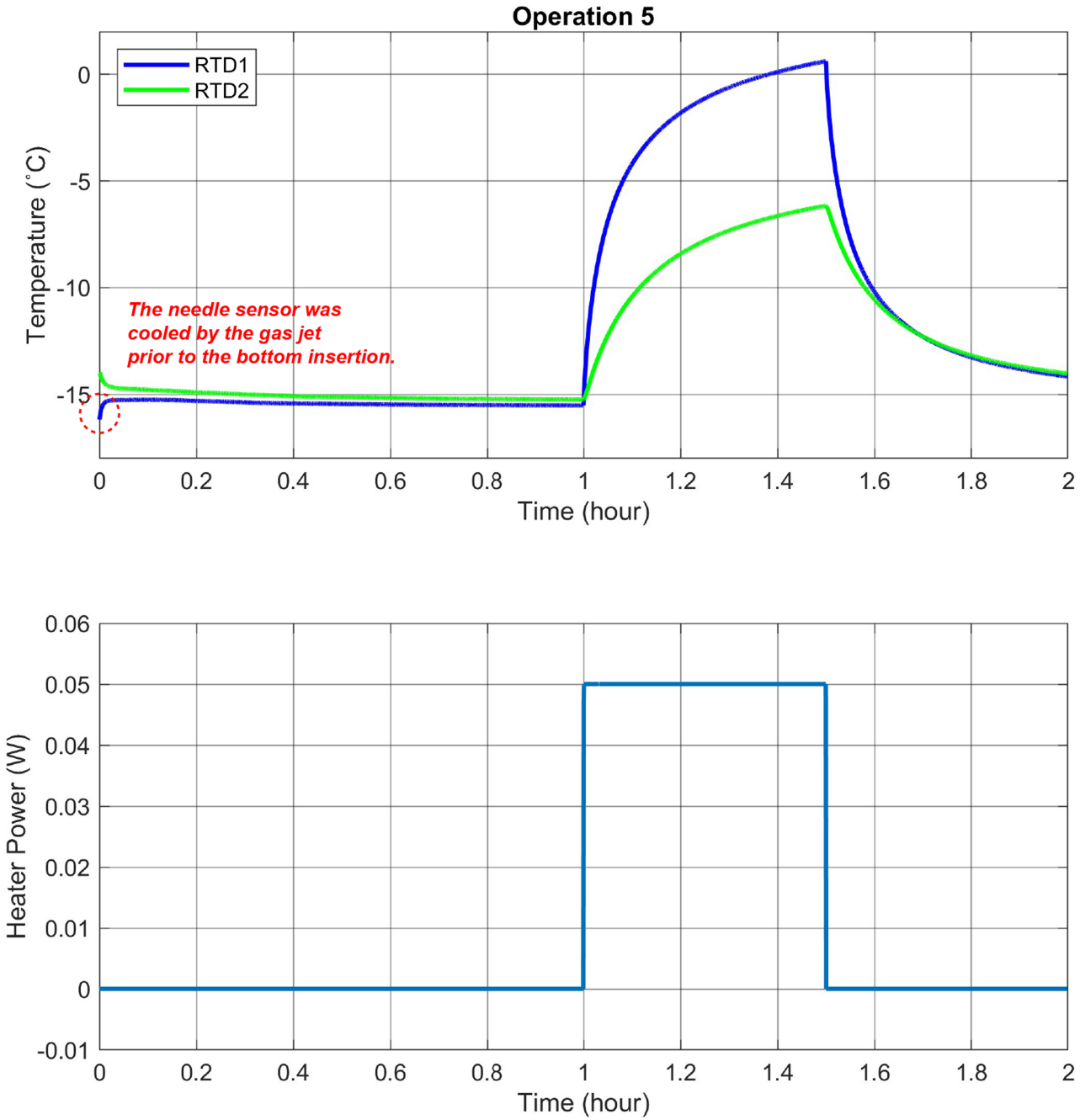

Figure 4. An example of the thermal measurements made by LISTER at one depth. Top: a graph of temperature vs. time (after bottom-hole regolith insertion) for the two RTDs in the needle sensor during operation 5 at 0.329 m depth. RTD1 was positioned at the midpoint of the needle, and RTD2 was positioned in the gas nozzle (Figure 2). For this operation, the sensor assembly was initially warmer than the bottom-hole regolith. During the excavation, the needle sensor was cooled by the adiabatic expansion of the gas emitted by the nozzle. After the bottom insertion (and the cessation of the gas jet), the temperature of the needle sensor warmed up to that of the regolith. That is what we see in the record of RTD1 in the first few minutes. RTD2 was less affected by the cold gas jet and thus initially warmer but cooled toward the regolith temperature after the bottom insertion. Bottom: heater power vs. time (after bottom-hole regolith insertion) of the needle sensor.

LISTER is designed to measure the temperature and thermal conductivity of the regolith at multiple depths (Figure 2). The sensor for these measurements ("needle sensor," 2.8 mm diameter and 28 mm length) is attached to the leading end of the S.S. tube. When the needle sensor reaches one of the subsurface depths targeted for thermal measurements, LISTER stops blowing gas and pushes it into the yet-to-be-excavated bottom-hole regolith.

The needle sensor contains two resistance temperature detectors (RTDs) and a coiled heater wire running along its length. LISTER monitors the temperature of the needle for 1 hr while it equilibrates with the surrounding regolith (Figure 4). Afterward, the heater is activated for 30 minutes, during which time the temperature of the needle rises. The magnitude of the temperature increase is indicative of the thermal conductivity of the regolith. The greater the magnitude is, the lower the thermal conductivity is, and vice versa. The actual determination of thermal conductivity is made by duplicating this heating experiment with a finite-element thermal model of the sensor assembly. This measurement method is similar to that

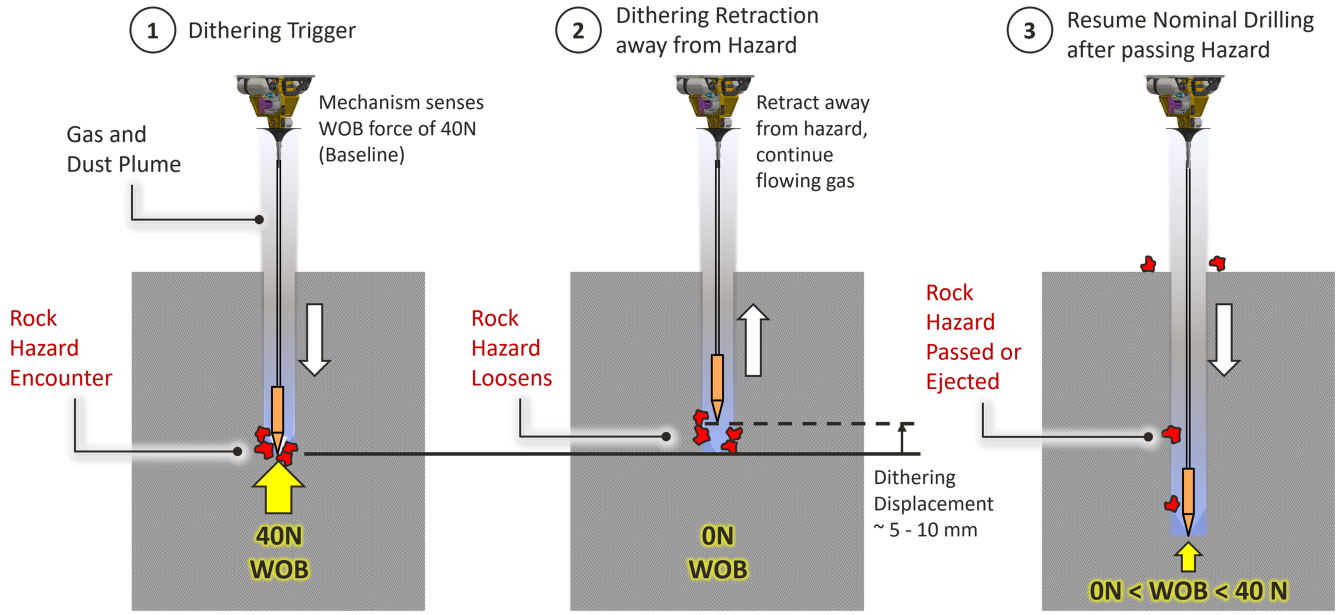

Figure 5. Conceptual drawings describing the dithering maneuver of LISTER.

used for the InSight mission (M. Grott et al. 2021). After the heating, the needle is allowed to cool off for 30 minutes. It takes a total of 2 hr to complete a full sequence of thermal measurements.

When the thermal measurements have been completed, LISTER resumes its subsurface descent toward the next targeted depth. Prior to resumption of the excavation, LISTER's sensor assembly is raised 1 cm above the bottom of the hole to ensure that the gas exit nozzles are not blocked.

LISTER detects the presence of obstacles on its way by monitoring the weight on bit (WOB). When the WOB exceeds a programmable threshold, it automatically performs a "dithering" maneuver, a piston-like, up-and-down movement with 5 or 10 mm amplitudes, while maintaining gas flow (Figure 5). By doing so, LISTER aims to release the WOB force from the obstacle and dislodge it. If dithering is triggered multiple times without sufficient downward progress (typically three up-and-down cycles while advancing less than 10 mm; set by operators), LISTER stops excavation and waits for the next operator command.

LISTER is designed to reach 3 m depth. On the Moon, the temperature of the regolith below ∼1 m depth is stable enough to yield the thermal gradient representative of the endogenic heat flow (M. G. Langseth et al. 1976). For that purpose, LISTER aims to make thermal measurements at multiple depths below 1 m depth. If LISTER does not quite reach beyond 1 m depth, which was the case for the Blue Ghost mission, the in situ thermal measurements made at shallower depths still enable us to build a thermal model of the regolith that reacts to the fluctuation of solar heat intake, from which the thermal gradient that represents the endogenic heat flow may be estimated (e.g., S. Nagihara 2023).

3. System Architecture

LISTER's mechanism consists of five subsystems (Figure 6): deployment, pneumatics, sensor, thermal control, and lander interface. The total mass, including the avionics, is 12.9 kg.

3.1. The Deployment Subsystem

Prior to deployment, the S.S. tube is coiled around the storage reel (Figure 7). The sensor assembly, attached to the leading end of the tube, is accommodated inside the probe tip housing below the storage reel housing. When deployment begins, the actuator, located between the storage reel housing and the probe tip housing, spins the drive roller. The leading end of the tube, squeezed between the drive roller and the counter roller, is then pulled downward. As the tube spools out of the storage reel, these two rollers and the intermesh roller above straighten it. The feed guides in the storage reel housing assist in the tube straightening. As the tube spools out, the sensor assembly emerges from the bottom of the probe tip housing.

The deployment subsystem tracks the rotation of the drive roller and estimates the length of the S.S. tube spooled out. This estimation has been calibrated within 1.2% in lab tests. When the needle sensor touches the ground surface for the first time, it is detected by an increase in the WOB force. The length of the tube that has been spooled out at that point is marked as zero depth.

During excavation, the WOB force detection algorithm is also used for triggering dithering. Fluctuation of the WOB force is tracked by monitoring the actuator current draw as a proxy, and the algorithm dynamically updates the dithering-triggering threshold while keeping the WOB below the safety threshold of 120 N. That minimizes the risk of premature triggering of dithering at a low WOB force.

3.2. The Pneumatics Subsystem

LISTER accommodates two nitrogen gas tanks below the lander interface structure and above the storage reel housing (Figures 2, 3, and 8). Predeployment, the gas tanks are pressurized at 30.3 MPa at room temperature. The pneumatics manifold feeds regulated gas into a flow-restricting orifice at the upper end of the S.S. tube. The gas is emitted through the holes located in the bottom of the spacer-nozzle assembly with a flow rate of ∼12 standard liters per minute (SLPM). Due to

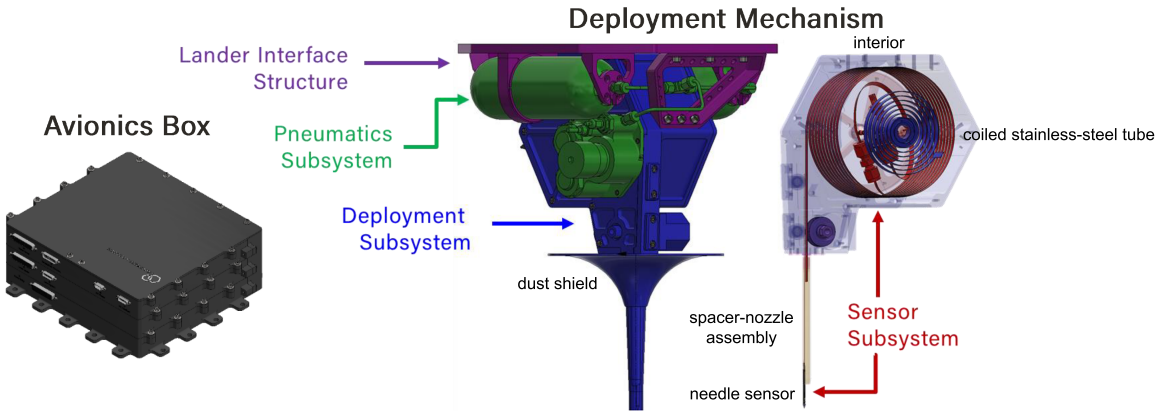

Figure 6. Drawings of the two major hardware components (the avionics box and the deployment mechanism). The subsystems of the deployment mechanism are color-coded (the middle diagram). The lander interface structure is in magenta. The pneumatic subsystem is in green. The deployment subsystem is in blue. The sensor subsystem is shown in a separate diagram (right).

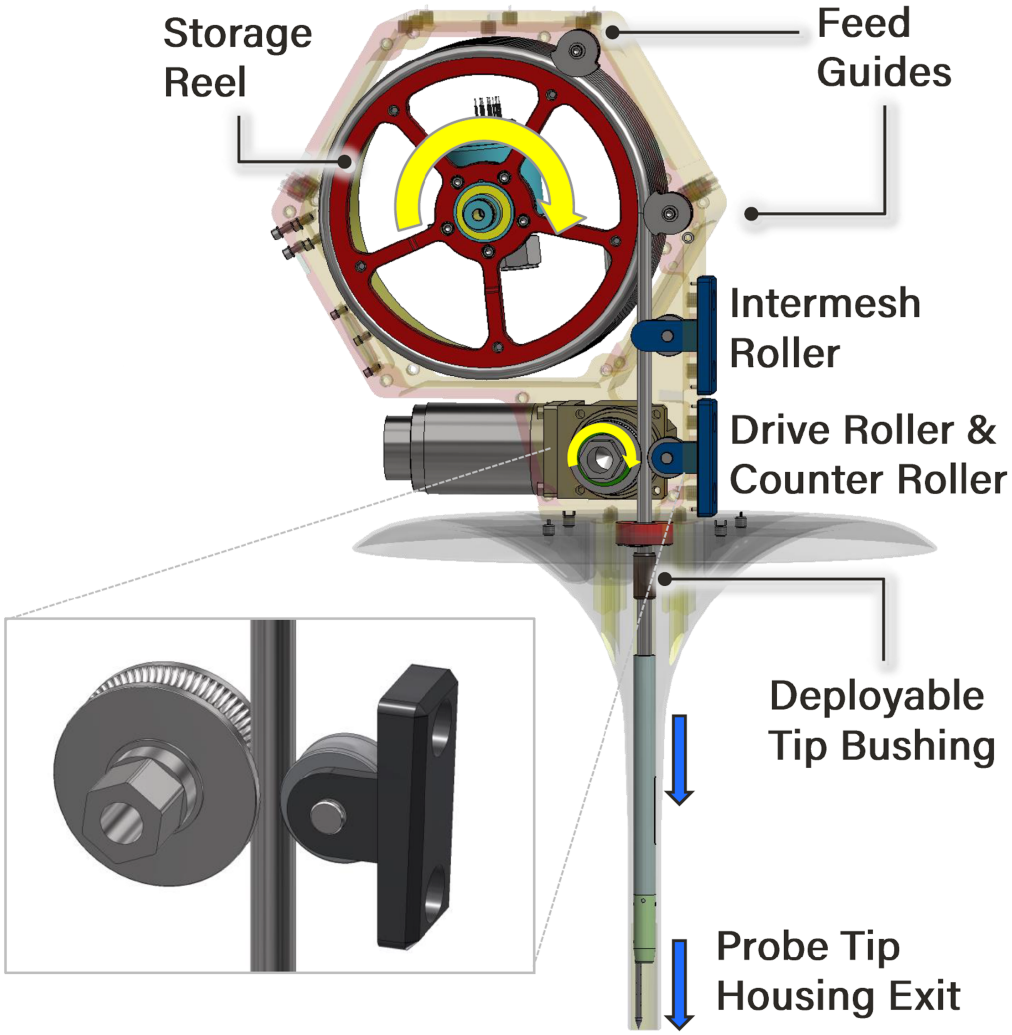

Figure 7. Drawings of the mechanism for spooling and straightening the S.S. tube of the deployment subsystem.

single-stage gas regulator behavior, as the tank pressure drops, the gas flow increases over time to ∼15 SLPM toward the end of life. Each gas tank holds 130 g of nitrogen gas, and that is sufficient for ∼12 minutes of normal excavation, twice the amount nominally needed. If the probe does not run into major obstacles, it takes ∼30 s to advance 0.5 m deeper into the regolith with the 12 SLPM flow rate based on our excavation tests using a prototype in vacuum chambers. A higher flow rate would improve excavation performance, but it would use up the gas faster.

A redundant O-ring sealing mechanism was used at the interfaces between the gas tanks and the pneumatic plumbing

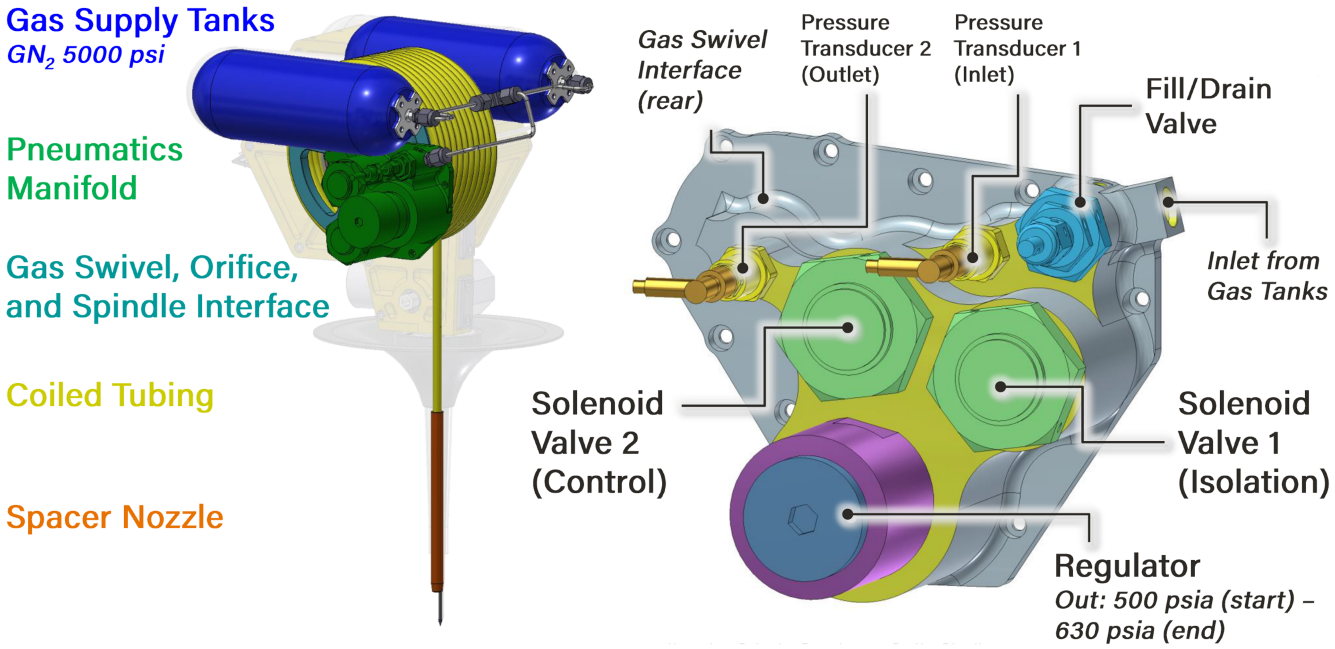

Figure 8. Left: an overview drawing of the pneumatic subsystem. Right: a drawing of the pneumatic manifold.

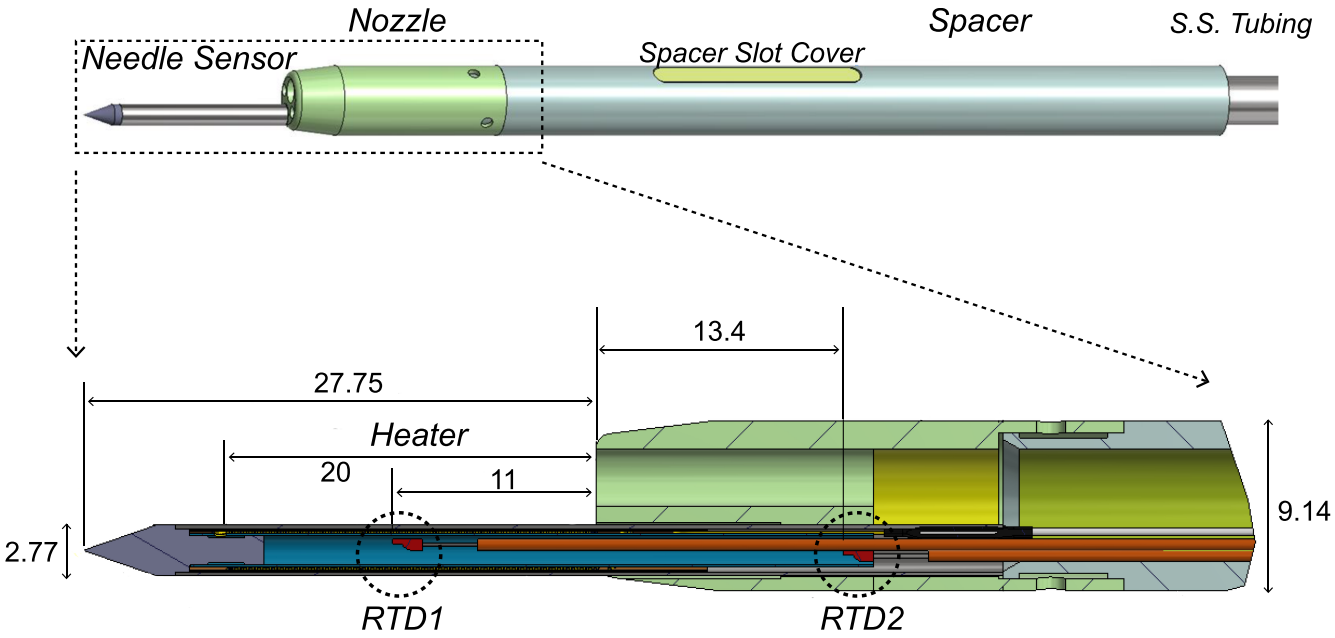

Figure 9. Top: a drawing of the exterior of the sensor subsystem. Bottom: a drawing of the internal construction of the needle sensor and the gas nozzle. The dimensions are in millimeters.

assembly (Figure 8) to minimize gas leaks. The tank gas pressure was monitored periodically during the transit to the Moon, and no significant drop was observed.

3.3. The Sensor Subsystem

The sensor subsystem consists of the needle sensor, the associated electrical components, and the spacer-nozzle assembly, which joins the sensor with the S.S. tubing (Figures 2 and 9). To minimize the heat exchange between the S.S. tube and the needle sensor, G10 CR fiberglass, a material of relatively low thermal conductivity ($0.6\ \mathrm{W\ m^{-1}\ K^{-1}}$), is used for the spacer and the nozzle (10 cm length and 1 cm O.D.).

The casing of the needle sensor (2.8 mm outside diameter and 28 mm exposed length) is S.S. There is another S.S. tube inside it ("inner needle"), and it houses a platinum RTD (RTD1). The inner needle is also wrapped by Manganin resistance wire, which generates the heat necessary for the thermal conductivity measurement. Its power is maintained at 50 mW, when active. The heater covers the full length of the needle probe, and RTD1 is positioned at its midpoint. A spare RTD is placed inside the inner needle at its joint with the spacer-nozzle assembly (RTD2). The RTDs are calibrated for

TRL 2	TRL 3	TRL 4	TRL 5	TRL 5	TRL 6	TRL 9
[2008]	[2009-10]	[2011]	[2012-14]	[2019]	[2019-2022]	[2022-2025]
50-cm in sand	1-m in Hawaiian tephra	1-m in JSC-1a in TVAC	2-m in NU-LHT-2M in TVAC	3-m in a lab	2-m in NU-LHT-2M in TVAC	1-m on the Moon
Tape measure	Tape measure	Fiberglass	Fiberglass	Fiberglass	Coiled Tubing	Coiled Tubing

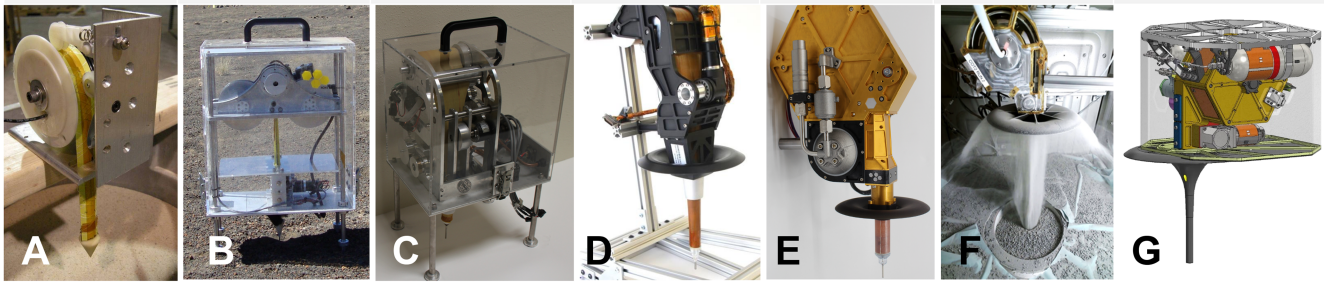

Figure 10. Photographs and a drawing of the earlier prototypes of LISTER.

0.01 K absolute temperature measurement accuracy for the range of temperatures expected for the subsurface of the landing site (S. Nagihara 2023). A 24 bit analog-to-digital converter is applied to the range of 100–400 K, which yields a temperature measurement resolution of better than 0.001 K.

LISTER's sensor subsystem is designed to minimize the time required for the subsurface measurement sequence. The use of the thin needle sensor and thermally decoupling it from the rest of the instrument hardware enables quick thermal equilibration with the surrounding regolith. The design facilitates rapid deployment into the subsurface.

3.4. The Thermal Control Subsystem

Thermal control is important in two aspects for LISTER. The first is to keep its mechanism and avionics within the optimum range of temperature for their survival and operation. The second is to minimize the temperature fluctuation of the above-the-ground hardware that may affect the measurements by the needle sensors underground.

The LISTER mechanism is mounted under the lander's deck to avoid direct sunlight (Figure 2). In addition, a curtain consisting of a multilayer insulation blanket hangs from the lander interface plate to block the low-angle sunlight. When the ambient temperature is low, the heaters within the mechanism and the avionics box will maintain their temperature at ∼30°C. If the ambient temperature rises above this, the heaters deactivate, and the temperature of the LISTER hardware follows that of the environment. Therefore, at a low-latitude landing site such as Mare Crisium, LISTER operations should be completed in the morning, before the lander's temperature goes well above 30°C.

3.5. The Lander Interface Subsystem

The design of the lander interface subsystem (Figure 6) depends somewhat on the lander. For the Blue Ghost mission, a thermal spacer was incorporated into the interface subsystem to achieve adiabatic coupling (0.1 W K^{-1}) with the lander's platform.

4. Development History

LISTER represents nearly two decades of technological development of robotically deployable subsurface probes starting in 2008. The proof of concept of pneumatic excavation was done with a system in which a pair of metal tapes were bound together in a biconvex form, through which a gas tube was fed. This tape bundle spooled out of a drum like a steel tape measure. A penetrating cone with a gas hole and a needle sensor were attached to the leading end of the tape bundle (Figure 10(A)). This system, representing a technology readiness level (TRL) of 2, was tested in a bucket of sand and for the first time demonstrated that excavating granular materials with gas is possible (E. Mumm et al. 2010). This system was further developed (Figure 10(B)) and successfully tested multiple times in Hawaiian tephra on the slopes of Maunakea volcano during 2010 NASA field testing and reached TRL 3 (K. Zacny et al. 2012). The next prototype (Figure 10(C)) replaced the metal tapes with fiberglass tapes, and it was successfully tested in a vacuum chamber in a compacted JSC-1a lunar soil simulant (X. Zeng et al. 2010), reaching TRL 4 (K. Zacny et al. 2013). At that point, our main effort shifted to scaling down the mass and making the system flight-like. This was achieved with the TRL 5 prototypes (Figures 10(D) and (E)), which weighed just over 2 kg and had a significantly smaller-diameter fiberglass stem. They were tested in a large vacuum chamber in an NU-LHT-2M lunar soil simulant (A. Slabic et al. 2024) to a depth of 2 m (K. Zacny et al. 2020).

In developing the flight system for the Blue Ghost mission, our main concern was to minimize the hole diameter, and hence the probability of its probe hitting subsurface rocks, while enhancing the robustness of the excavation system. To do so with the fiberglass tapes proved difficult. A new trade was done, and the coiled metal tubing approach, already under development at Honeybee Robotics for another project, was adopted (B. Mellerowicz et al. 2022). The diameter of the new S.S. tube was 6.4 mm, one-fourth of the 25.4 mm of the previous fiberglass stem. The thin-diameter tube also used less gas. In addition, the S.S. tube offered significant rigidity and allowed higher WOB forces with reduced buckling (Figures 10(F) and (G)).

5. Excavation Operations in Mare Crisium

The Blue Ghost lander touched down in Mare Crisium (18.°5623N and 61.°8103E) at the local dawn on 2025 March 2 and ended its mission shortly after sunset on March 16. LISTER operated on March 4–6 (Figure 11) and then rested for several days while the temperature of the lander exceeded

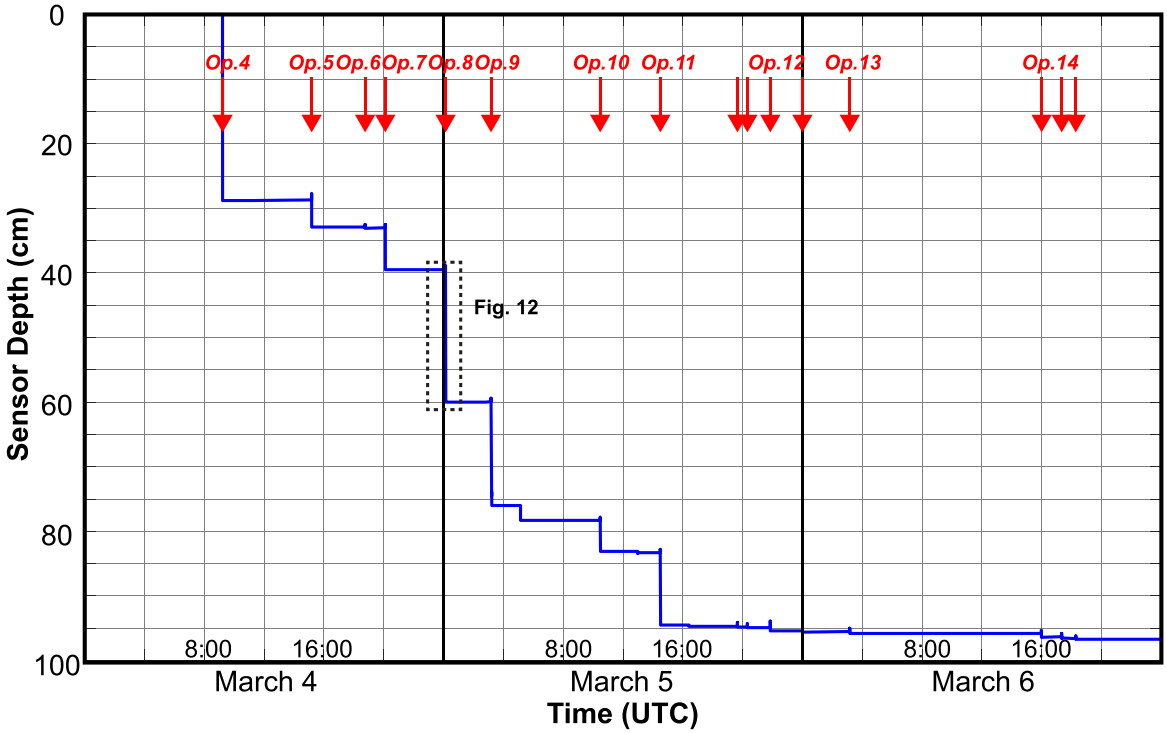

Figure 11. A graph of LISTER's sensor depth vs. time during the surface operations. The timings of excavation operations are indicated by the red arrows.

the upper limit of the operational temperatures for most of its payloads. Afterwards, LISTER operated for 2 more days toward the end of the mission. LISTER reached 98 cm depth during the first 3 days of operations and then hit major obstacles at that depth. We were not able to overcome the obstacles during the second half of the operations. Because this article focuses on the regolith excavation, we mainly describe the data from the first 3 days of operations.

We define one sequence of excavating regolith and carrying out thermal measurements as one "operation." The first three operations were used to establish the zero depth, where the midpoint of the needle sensor was positioned at the surface. For operation 4, LISTER was commanded to penetrate to 29 cm depth and carry out thermal measurements, and this was successfully executed. For the subsequent operations, LISTER was commanded to excavate 0.5 m deeper each time but stopped short by running into obstacles (Figure 11). From operations 6 to 11, by using various combinations of dithering, pushing, and gas blowing, LISTER overcame these obstacles and advanced deeper. However, starting with operation 12, LISTER could advance only 1–2 cm at a time. We halted after operation 18, because LISTER no longer advanced deeper.

Every time an excavation operation was halted, temperature and thermal conductivity measurements took place at that depth, if the needle sensor advanced more than ∼0.1 m deeper than its previous position (operations 4–11; Figure 11). Once LISTER reached ∼0.95 m depth, each excavation operation yielded progress of only 0.01–0.02 m, and thermal measurements were taken less frequently. In the end, the measurements were taken at eight depths for operations 4 (0.288 m), 5 (0.329 m), 7 (0.394 m), 8 (0.6 m), 9 (0.783 m), 11 (0.947 m), 12 (0.956 m), and 18 (0.971 m). Figure 4 is a good representative of the thermal data we acquired at each depth. A more detailed description and analysis of these data are given in a separate article, because the focus of this article is on the regolith excavation.

What caused LISTER to stop short before reaching its commanded depth cannot be known for certain, and it may well vary among the individual operations. Given that LISTER was able to overcome the obstacles that halted the previous run on several occasions suggests that it may have simply needed more gas blowing to flush the hole more thoroughly or more dithering to dislodge the obstacles. LISTER can loosen semiconsolidated regolith, but not solid rocks, because it does not have a conventional drill bit. After operation 11, the downward progress halted, probably because stones too large/heavy to be blown out of the hole accumulated at the bottom of the hole, and they could no longer be pushed aside.

Even though LISTER did not advance beyond 1 m depth, the dithering maneuver proved effective. Here are some examples. Operation 7 halted at 39 cm depth (Figure 11) because LISTER ran into an obstacle, which could not be overcome after a round of dithering. For operation 8, we commanded LISTER to repeat multiple rounds of dithering, in case it could not overcome the obstacle after one round. After two rounds of dithering, LISTER resumed its downward advance. Before it halted at 60 cm depth, it engaged in dithering several more times to keep going (Figure 12).

We also observed that the repeated gas blowing through these excavation operations made the hole gradually wider and more circular (Figure 13). After our first excavation (operation 4), the diameter of the hole at the surface was ∼2 cm. After the last operation, the surface hole diameter was ∼7 cm, consistent with what was achieved in preflight vacuum chamber tests. Even though the camera does see deep inside, the hole likely becomes narrower with depth, as the vacuum chamber tests also showed.

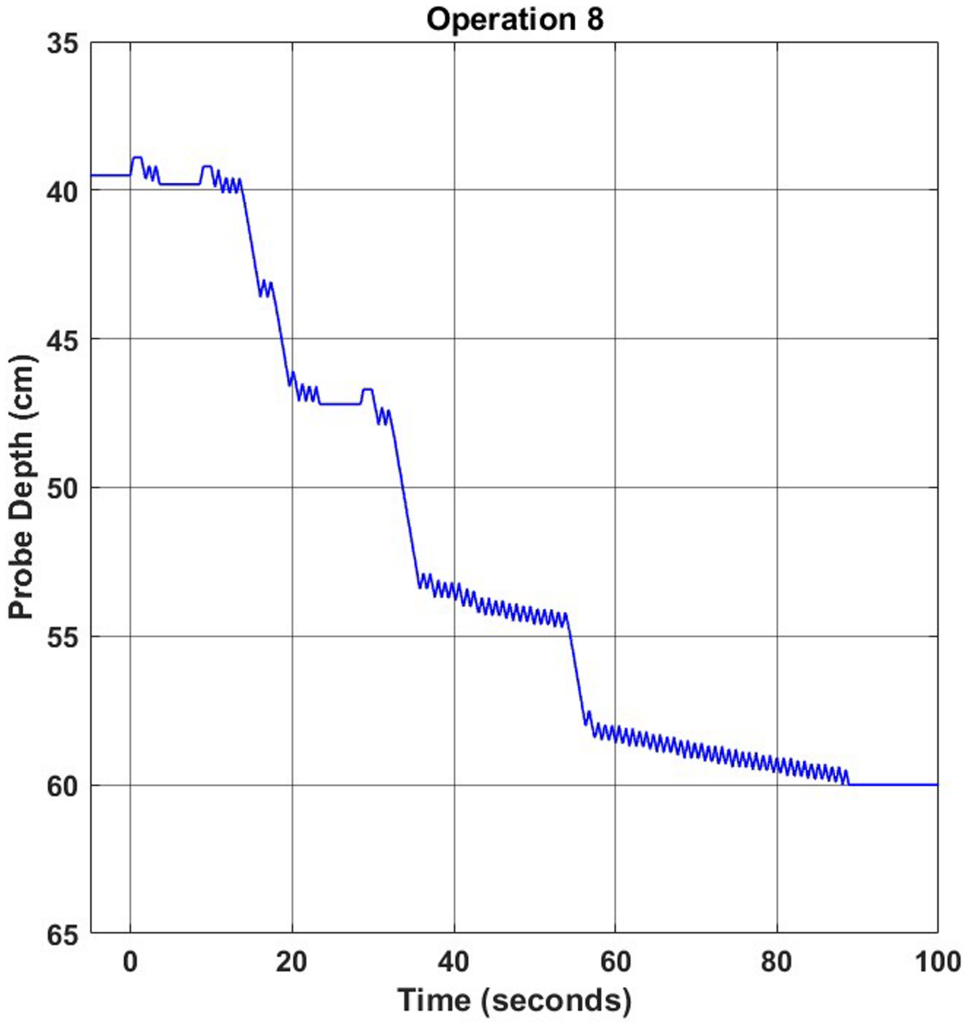

Figure 12. A graph of LISTER's sensor depth vs. time for operation 8. The zigzags indicate occurrences of the dithering maneuver.

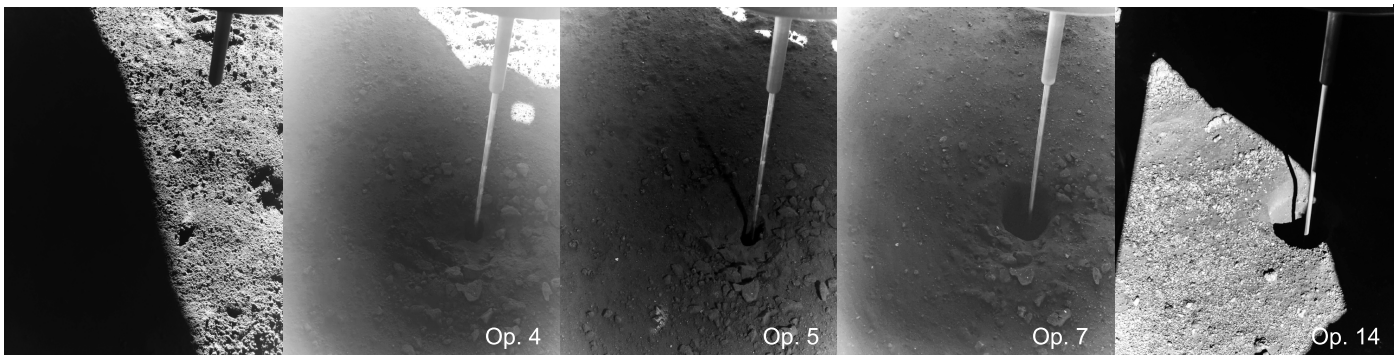

Figure 13. Photographs of the ground below LISTER before excavation (left) and the hole excavated by LISTER after operations 4, 5, 7, and 14, captured by the Argus 8 below-deck camera. See Figure 10 for the timings of these operations. See Figure 14 for the position of the camera. Recall that the diameter of the S.S. tube is 6.4 mm for scale.

6. Implications for the Surface Geology of the Landing Site

Recording LISTER's operations on video cameras (Figure 14) also proved useful for studying the geology of the regolith excavated. For example, during operation 4, we observed textural changes in the materials ejected several times in the first ∼10 s of excavation (Figure 15). The most notable were explosive ejections of clasts that happened twice. They resembled eruptions of composite volcanoes. Each time, the explosion was led by an eruption plume of fine-grained, optically reflective particles (Figures 15(B) and (D)), followed by clastic projectiles (Figures 15(C) and (E)). The second explosion was considerably larger.

We believe that each of the explosions was associated with a bed of regolith breccia (aka soil breccia). Regolith breccias form from low-impact lithification of local lunar soil in a

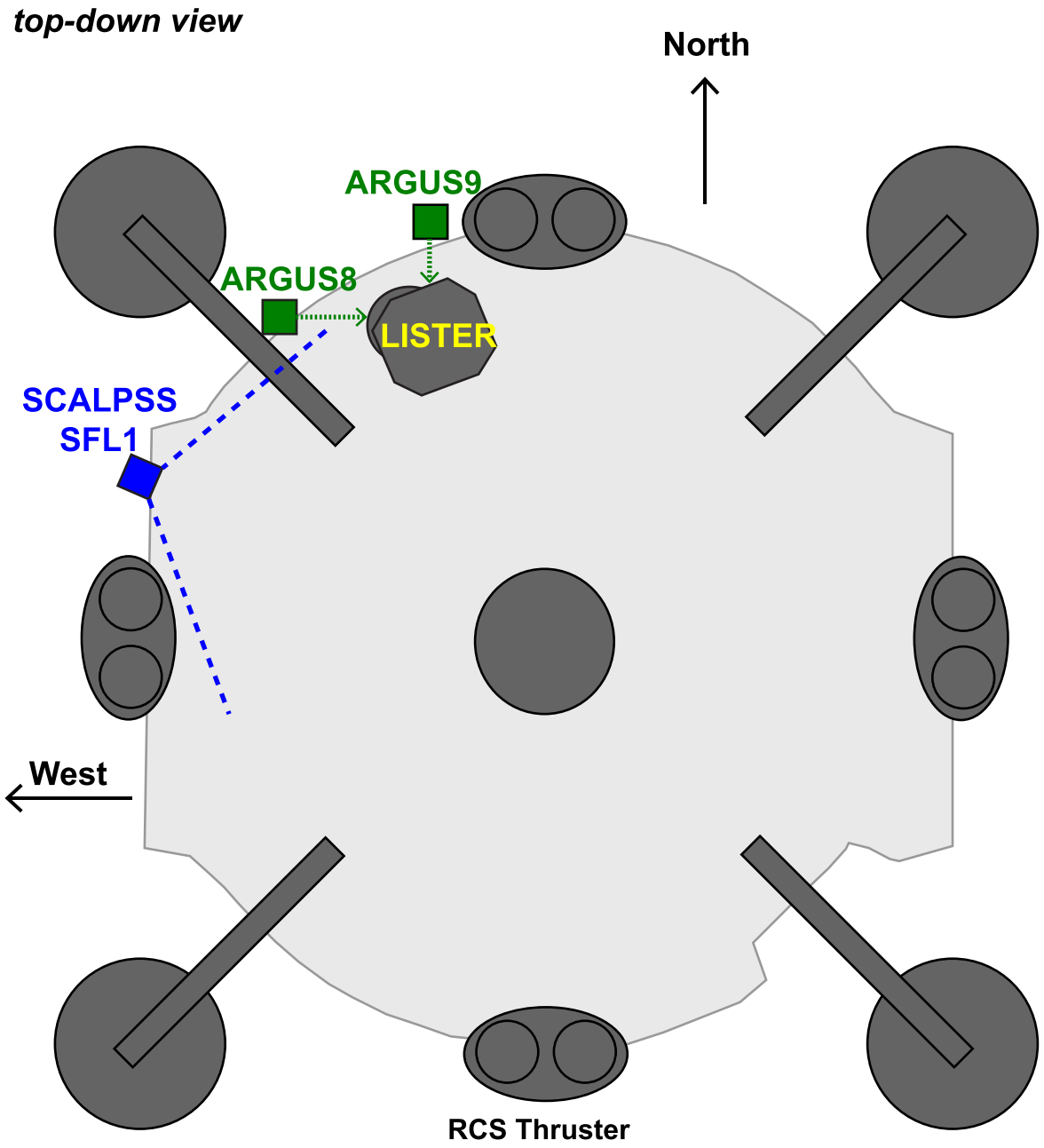

Figure 14. A top-down view drawing of the positions of the below-deck cameras used to monitor LISTER's operations. Argus 8 and 9 are video cameras operated by Firefly Aerospace. SFL1 is a wide-angle, short-focus black-and-white camera of the SCALPSS payload. The blue dashed lines indicate its field of view.

shallow subsurface (J. F. Lindsay 1976; D. S. McKay et al. 1991). They are not fully lithified and tend to be friable. Due to the lithification, regolith breccias are much less permeable to gas than noncohesive soils. When LISTER encountered a bed of regolith breccia, the initial contact by the needle sensor tip likely made some cracks. As the needle fully pushed through, the gas pressure likely built up beneath the impermeable bed. Eventually, the gas pressure overcame the overburden and the flexural rigidity of the bed and resulted in an explosion. The preceding eruptive plume probably consisted of fine glass particles, which are common for shock-sintered breccias (G. J. Taylor et al. 1991; J. G. Spray 2016).

Based on the timings of the explosions (Figure 15), we estimate that the upper bed of regolith breccia was ∼3 cm deep. Based on the duration of the explosion and the size of the ejected clasts, we estimate that this bed was less than 1 cm thick. The lower bed is estimated to be ∼9 cm deep and 1–2 cm thick. LISTER dithered once ∼6 s into the operation, and this may have been due to the needle tip contacting the lower regolith breccia bed.

Regolith breccias are common in lunar maria (R. M. Fruland 1983; G. J. Taylor et al. 1991). The beds LISTER encountered probably occupy wide areas around the landing site. Lithified regolith can be seen underneath the Blue Ghost lander (Figure 16). That is very likely the upper unit of regolith breccia LISTER penetrated. Similar observations were made previously in the areas where loose surface soils were removed by the landing of the Apollo lunar modules (P. T. Metzger et al. 2011).

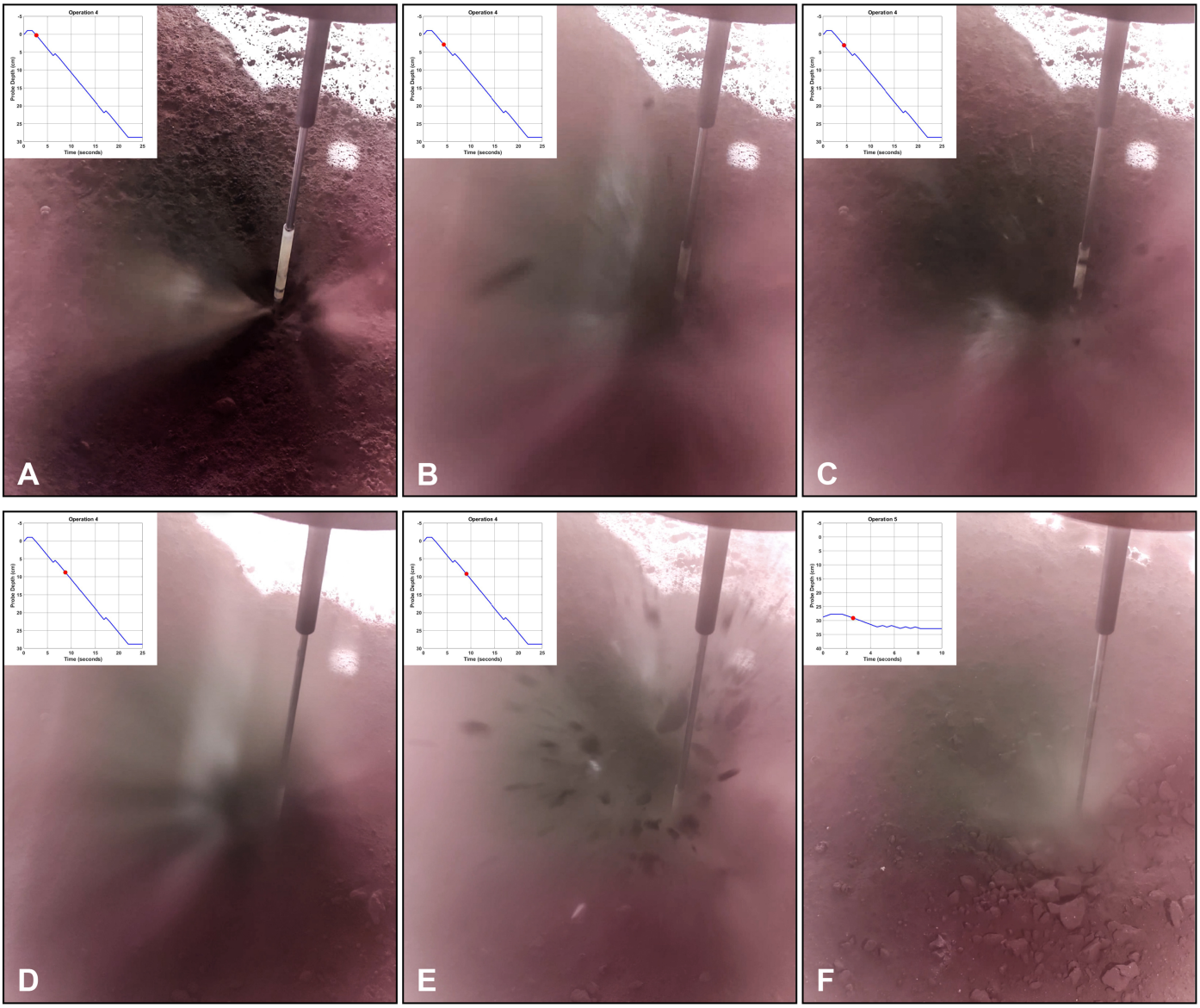

Figure 15. A series of snapshots obtained by Argus 8 during operations 4 (A–E) and 5 (F). The depth of the needle sensor is indicated by the red dot in the graph in the upper left corner of each photo. Photo A shows the very beginning of the excavation. Photo B captured the eruption plume of fine-grained reflective particles that preceded the first explosion captured in photo C. Photo D captured the eruption plume that preceded the second, larger explosion. Photo E captured the projectiles ejected by the second explosion. Photo F was taken during operation 5.

7. Discussion

Had we done anything different, could LISTER have penetrated deeper than 1 m into the regolith? One of the lessons we learned on the Blue Ghost mission is that there was plenty of reserve gas left in the tanks after completing the 14 initially planned operations. In hindsight, we could have run the gas jets with higher flow rates. Our previous tests in vacuum chambers showed that a higher gas flow rate would yield a larger hole and could blow out larger clasts. Unfortunately, in the current configuration, LISTER's gas flow rate is fixed and cannot be changed after launch. The current flow rate of ∼12 SLPM was set conservatively by balancing excavation performance and anticipated drawdown on each operation. For future missions, it should be possible to make minor modifications to enable adjustment of the gas flow rate by command.

Another lesson from the Blue Ghost mission is that, even if LISTER's subsurface advance falls short of reaching the commanded target depth by running into an obstacle, in some instances, we have been able overcome it by trying various combinations of dithering, gas blowing, and pushing. That suggests that there is some room for optimization of the parameters involved in dithering or triggering it, such as the WOB threshold, the speed, and the amplitude of dithering.

Finally, capturing LISTER's excavation operations on video increased the scientific return from this mission. Originally, the cameras were going to be used to detect any anomaly with LISTER operations, such as the S.S. tube bending or not going into the soil vertically. On future missions, imaging LISTER's ejecta plume with a spectroscopic camera would further enhance our ability to determine the mineral composition of the ejecta and the stratigraphy of the regolith of the landing site.

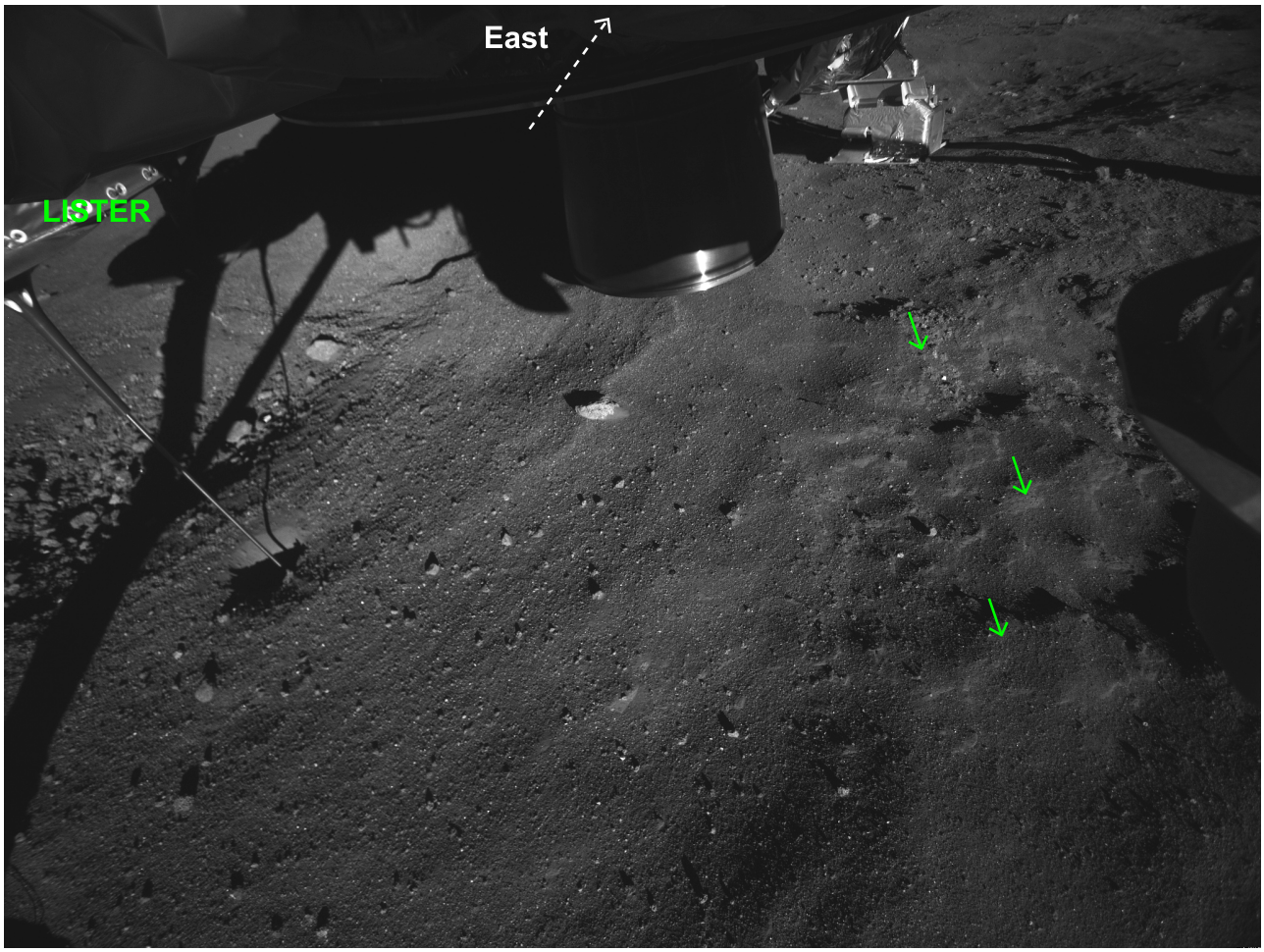

Figure 16. A photograph of the lunar surface below the lander obtained by camera SFL1 of the SCALPSS payload toward the end of the surface mission. See Figure 14 for the camera position and the field of view. The green arrows point to lithified materials exposed on the surface. They are likely regolith breccia. Courtesy of the SCALPSS team (O. K. Tyrrell et al. 2022).

8. Conclusions

The scientific importance of endogenic heat flow measurement on the Moon has been recognized since the Apollo era (e.g., M. G. Langseth et al. 1976; National Academies of Sciences, Engineering, and Medicine 2023). Like many other types of geophysical data, heat flow needs to be measured in situ at multiple locations on the Moon. Relying on human missions to do so has not been practical for expanding the geographic coverage of the data points. However, it has been a major technical challenge to robotically deploy a probe to a deep enough subsurface (>1 m) for endogenic heat flow measurement within the constraints of lander missions. LISTER on Blue Ghost Mission 1 has demonstrated for the first time that it is possible to pneumatically excavate lunar regolith to 1 m depth and collect thermal measurements at multiple depths. There is certainly room for improvement for future missions, such as being able to adjust the gas flow rate and fine-tuning the dithering maneuver. But, overall, we may have found in LISTER the system architecture and the concept of operations that would enable endogenic heat flow measurements on short-duration robotic lander missions to the Moon such as the ones currently conducted under NASA's CLPS program. At the minimum, with LISTER, we have made a major step forward in that direction.

Acknowledgments

Mike Selby and Sherry Jennings of the NASA Marshall Space Flight Center oversaw the development and delivery of LISTER. Mark Dillard of the NASA Johnson Space Center oversaw the delivery and spacecraft integration of LISTER. Farah Zuberi and Angus Fraser of Firefly Aerospace managed the integration and the lunar surface operations of LISTER. Maria Banks of the NASA Goddard Space Flight Center was the project scientist for the Blue Ghost mission. The below-deck camera images used for Figures 13 and 15 were provided by Firefly Aerospace. The below-deck camera image used for Figure 16 was provided by the SCALPSS payload team. We thank Paul Morgan for his contributions to an early stage of development. The work presented here was supported by the Lunar Surface Instrument and Technology Payloads program of NASA (contracts 80MSFC20C0022 to Texas Tech University and 80NM0020F0035 to the Jet Propulsion Laboratory, California Institute of Technology).

Data Availability

Data associated with the figures of this manuscript are currently peer-reviewed for archiving with NASA's Planetary Data System Geosciences Node. The data package is expected to be released to the public by the end of 2025 October (doi:10.17189/tyf3-jm93).

References

Banks, M. E., Barney, C., Buhler, C., et al. 2022, LPSC, 53, 2846
Barsukov, V. L. 1977, LPSC, 8, 3308
Carrier, W. D., III, Olhoeft, G. R., & Mendell, W. 1991, in Lunar Sourcebook, ed. G. H. Heiken, D. T. Vaniman, & B. M. French (Cambridge: Cambridge Univ. Press), 475
Firefly Aerospace 2025, Firefly's Blue Ghost Mission 1, https://fireflyspace.com/missions/blue-ghost-mission-1/
Fruland, R. M. 1983, Regolith Breccia Workbook (Washington, DC: NASA) https://www.lpi.usra.edu/lunar/samples/RegolithBrecciaWorkbook.pdf
Grott, M., Helbert, J., & Nadalini, R. 2007, JGRE, 112, E09004
Grott, M., Spohn, T., Knollenberg, J., et al. 2021, JGRE, 126, e06861
Heiken, G., & McEwen, M. C. 1972, EPSL, 17, 3
Keihm, S. J. 1984, Icar, 60, 568
Langseth, M. G., Keihm, S. J., & Peters, K. 1976, LPSC, 7, 3143
Lindsay, J. F. 1976, Lunar Stratigraphy and Sedimentology (New York: Elsevier)
Mathew, N., Durga Prasad, K., Mohammad, F., et al. 2025, NatSR, 15, 7535
McKay, D. S., Heiken, G., Basu, A., et al. 1991, in Lunar Sourcebook, ed. G. H. Heiken, D. T. Vaniman, & B. M. French (Cambridge: Cambridge Univ. Press), 285
Mellerowicz, B., Zacny, K., Palmowski, J., et al. 2022, NewSp, 10, 166
Metzger, P. T., Smith, J., & Lane, J. E. 2011, JGRE, 116, E06005
Mumm, E., Zacny, K., Kumar, N., et al. 2010, LPSC, 41, 2128
Nagihara, S. 2023, PSJ, 4, 166
National Academies of Sciences, Engineering, and Medicine 2023, Origins, Worlds, and Life: A Decadal Strategy for Planetary Science and Astrobiology 2023-2032 (Washington, DC: The National Academies Press)
Schloerb, F. P., Muhleman, D. O., & Berge, G. L. 1976, Icar, 29, 329
Siddiqi, A. A. 2018, Beyond Earth: A Chronicle of Deep Space Exploration, 1958–2016 (Washington, DC: NASA Office of Communications) https://www.nasa.gov/history/history-publications-and-resources/nasa-history-series/beyond-earth/
Siegler, M. A., Feng, K., Lehman-Franco, J. C., et al. 2023, Natur, 620, 116
Siegler, M. A., Smrekar, S. E., Grott, M., et al. 2017, SSRv, 211, 259
Slabic, A., Gruener, J. E., Kovtun, R. N., et al. 2024, Lunar Regolith Simulant User's Guide: Revision A 20240011783, NASA
Spohn, T., Grott, M., Smrekar, S. E., et al. 2018, SSRv, 214, 96
Spohn, T., Hudson, T. L., Marteau, E., et al. 2022a, SSRv, 218, 72
Spohn, T., Hudson, T. L., Witte, L., et al. 2022b, AdSpR, 69, 3140
Spohn, T., Seiferlin, K., Hagermann, A., et al. 2007, SSRv, 128, 339
Spray, J. G. 2016, AREPS, 44, 139
Taylor, G. J., Warren, P., Ryder, G., et al. 1991, in Lunar Sourcebook, ed. G. H. Heiken, D. T. Vaniman, & B. M. French (Cambridge: Cambridge Univ. Press), 183
Tyrrell, O. K., Thompson, R. J., Danehy, P. M., et al. 2022, in AIAA SCITECH 2022 Forum, 1693
Vinogradov, A. P. 1971, LPSC, 2, 1
Zacny, K., Currie, D., Paulsen, G., et al. 2012, P&SS, 71, 131
Zacny, K., Nagihara, S., Hedlund, M., et al. 2013, EM&P, 111, 47
Zacny, K., Paulsen, G., Chu, P., et al. 2020, in Advances in Terrestrial and Extraterrestrial Drilling, ed. Y. Bar-Cohen & K. Zacny, Vol. 2 (Boca Raton, FL: CRC Press)
Zeng, X., He, C., Oravec, H., et al. 2010, JAerE, 23, 111
Zhang, T., Pang, Y., Zeng, T., et al. 2023, IJRR, 42, 586
Zheng, Y., Yang, M., Deng, X., et al. 2023, ChJA, 36, 292